Earthq Eng & Eng Vib (2009) 8:165-177 **DOI**: 10.1007/s11803-009-9043-2

Preliminary analysis of the hanging wall effect and velocity pulse of the 5.12 Wenchuan earthquake

Liu Qifang† and Li Xiaojun‡

Institute of Engineering Mechanics, China Earthquake Administration, Harbin 150080, China

Abstract: A preliminary study of the PGA attenuation, hanging wall effect and velocity pulse characteristics from the 2008 Wenchuan earthquake of M_s =8.0 is described in this paper. The study was carried out through analyses in the time and frequency domains of main earthquake records. In the PGA attenuation study, records from 316 stations less than 1000 km from the surface rupture of the fault were used as a database and attenuation relationships were developed and compared with some existing relationships that are widely used in mainland China, Chinese Taiwan and the US. At the same time, records from 28 stations less than 100 km from the fault were used to study the hanging wall effect and velocity pulse characteristics of this earthquake based on the distribution of PGA, PGV, spectral acceleration, and the velocity pulse peak, and the results are compared with the 1999 Chi-Chi earthquake. In addition, the large PGAs of the UD components observed in this event are also discussed in this paper. From the results of the preliminary study, some conclusions are developed and suggestions for further research are proposed.

Keywords: Wenchuan earthquake; hanging wall effect; velocity pulse; attenuation

1 Introduction

At 14:28 on May 12, 2008 (Beijing time), an M_s = 8.0 earthquake struck South China. The earthquake epicenter was located at latitude 31.021ºN, longitude 103.367ºE, Wenchuan, Sichuan Province. Field investigations and an earthquake source inversion study (Chen *et al.*, 2008; Wang *et al.*, 2008, Xu *et al.*, 2008) showed that the devastating earthquake ruptured unilaterally from southwest to northeast with a rupture length at the ground surface of about 240 km along the Beichuan-Yingxiu fault and 72 km along the Guanxian-Jiangyou Fault (Xu *et al.*, 2008).

During the main earthquake, about 1,400 components of acceleration records were obtained from 460 stations (including an array for topographical effects observation) in 17 provinces by the China National Digital Strong Motion Observation Network System (Li *et al.*, 2008a; 2008b). These strong motion data provided useful information for studying earthquake source mechanisms and other earthquake engineering related issues. This paper focuses on a preliminary study of acceleration attenuations, hanging wall effect and velocity pulse characteristics observed in this earthquake by using data from selected stations.

Correspondence to: Liu Qifang, Institute of Engineering Mechanics, China Earthquake Administration, 9 Xuefu Road, Harbin 150080, China
Tel: +86-451-86652622
E-mail: Qifang_liu@126.com
†Associate Professor; ‡Professor

Supported by: National Natural Science Foundation of China Under Grant No. 90715038; National Basic Research Program of China Under Grant No. 2007CB71420); the Basic Science & Research Foundation of Institute of Engineering Mechanics, CEA Under Grant No. 2006A02
Received March 23, 2009; **Accepted** April 15, 2009

2 Data selection

The fault distance is defined as the closest distance from a station to the surface rupture of the Beichuan-Yingxiu fault. As PGAs from records of most stations more than 1,000 km from the fault were less than 10 Gal, they had little influence on the attenuations. Therefore, 316 stations located less than 1,000 km from the fault were selected for this study. Figure 1 shows the distribution of these stations.

28 stations were less than 100 km from the fault and were used to study the characteristics of near-fault strong motions. Among these 28 stations, 11 were located on the hanging wall and 17 on the footwall. Of these, two stations on the hanging wall and three stations on the footwall were located on rock sites, while all the others were on soil sites. Figure 2 shows the distribution of these stations, and Table 1 summarizes the values of PGA, PGV, and spectral accelerations at periods 0.1 s, 0.5 s, 1.0 s and 3.0 s, respectively.

3 Attenuations of PGAs

Before the 5.12 Wenchuan earthquake, only a

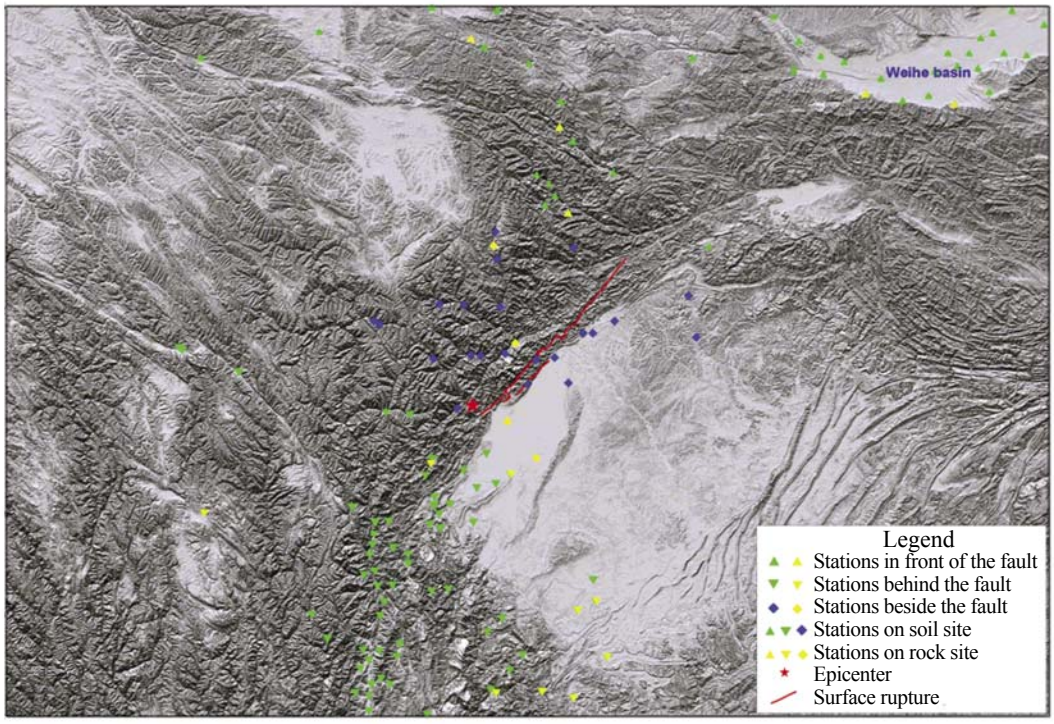

Fig. 1 Distribution of strong motion stations in fault distances less than 1000 km that provide data used in the attenuation study

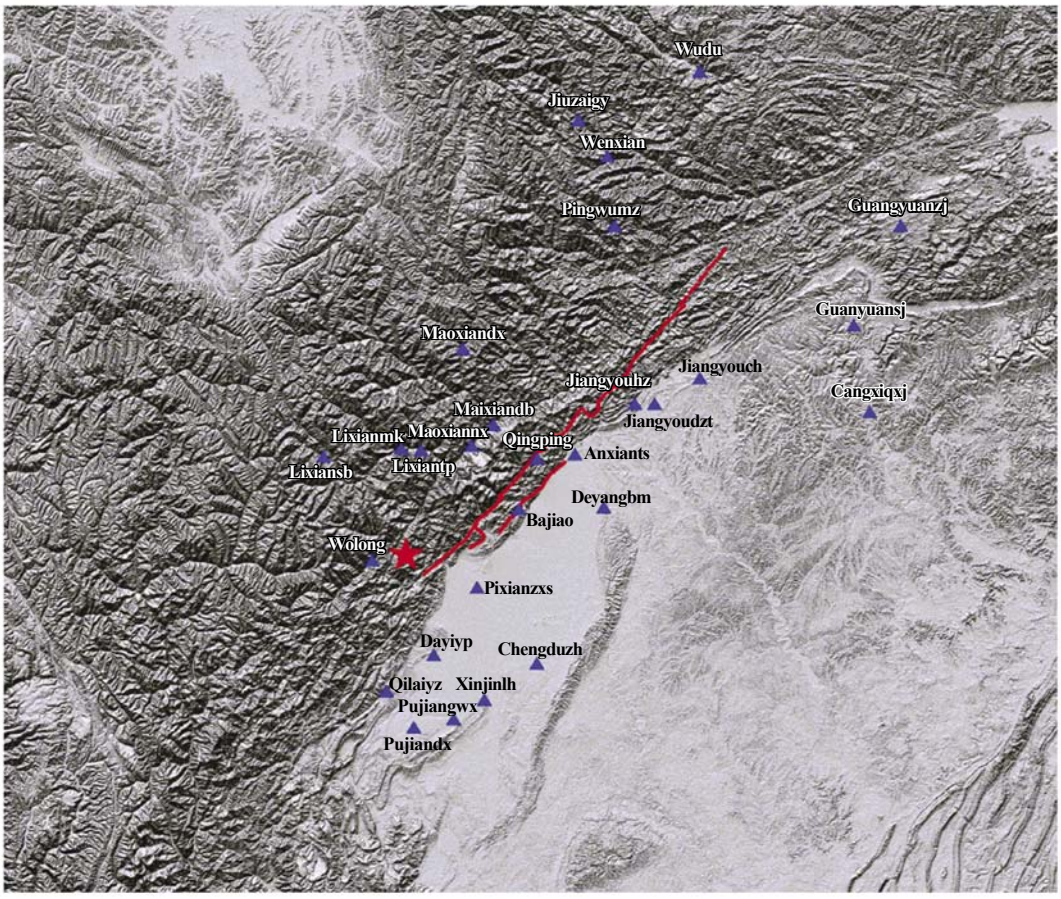

Fig. 2 Distribution of stations with fault distances less than 100 km used for near-fault motion feature study

few strong motion data in mainland China had been obtained from earthquakes with M_s >7.0. The large number of records in this earthquake provides an excellent opportunity to study the attenuations of large earthquakes in China and examine the availability of existing attenuation relationships. Figure 3 plots the recorded results along with attenuation relationships derived by curve-fitting for EW, NS and UD components, respectively, expressed as:

$$\lg a_{\mathrm{EW}} = 5.5577 - 1.5761\lg(D_{\mathrm{rup}} + 49.3767)$$
$$\sigma_{\lg} = 0.3740 \quad (1)$$

$$\lg a_{\mathrm{NS}} = 5.0194 - 1.3648\lg(D_{\mathrm{rup}} + 38.5396)$$
$$\sigma_{\lg} = 0.3890 \quad (2)$$

$$\lg a_{\mathrm{UD}} = 6.3430 - 2.0108\lg(D_{\mathrm{rup}} + 56.2397)$$
$$\sigma_{\lg} = 0.2976 \quad (3)$$

where a_{EW}, a_{NS} and a_{UD} denote the PGAs in EW, NS and UD directions, respectively; D_{rup} is the fault distance, and $\sigma_{\lg}$ is the standard deviation.

In Fig. 3, some other widely used relationships in mainland China, Chinese Taiwan, the west America and other parts of the world are provided for comparison purposes.

The relationship used in mainland China (Huo, 1989):

$$\lg a_{\mathrm{PG}} = -1.662 + 1.381M - 0.054M^2 - 1.938\lg(D + 0.3268\mathrm{e}^{0.615M}) \quad (4)$$

The relationship proposed by Chin-Hsiung Loh (from Hu, 1999) used in Chinese Taiwan

$$\ln a_{\mathrm{PG}} = -4.920 + 1.024M - 1.065\ln(D + 0.3095\mathrm{e}^{0.92M}) \quad (5)$$

The relationship used in the western USA (Joyner and Boore, 1981)

$$\ln a_{\mathrm{PG}} = -2.349 + 0.573M - \ln R - 0.00587R$$
$$R^2 = D^2 + 7.3^2 \quad (6)$$

and the relationship used in the world (Campbell, 1981)

$$\ln a_{\mathrm{PG}} = -4.1414 + 0.868M - 1.09\ln(D + R_0(M))$$
$$R_0(M) = 0.0606\mathrm{e}^{0.7M} \quad (7)$$

where a_{PG} denotes the PGA; D is the fault distance, and M is the surface wave magnitude.

Note that the vertical component attenuates more rapidly than the two horizontal components, which is consistent with historical earthquakes. Comparing the two horizontal attenuations, the PGAs of the EW components attenuate a little more rapidly than those of the NS components. This phenomenon may be related to the source mechanism, which should be studied further. As the fault distance becomes greater than 200 km, a meaningful phenomenon was observed; that is, PGA from most of stations in front of the fault were higher than from behind the fault at the same fault distance.

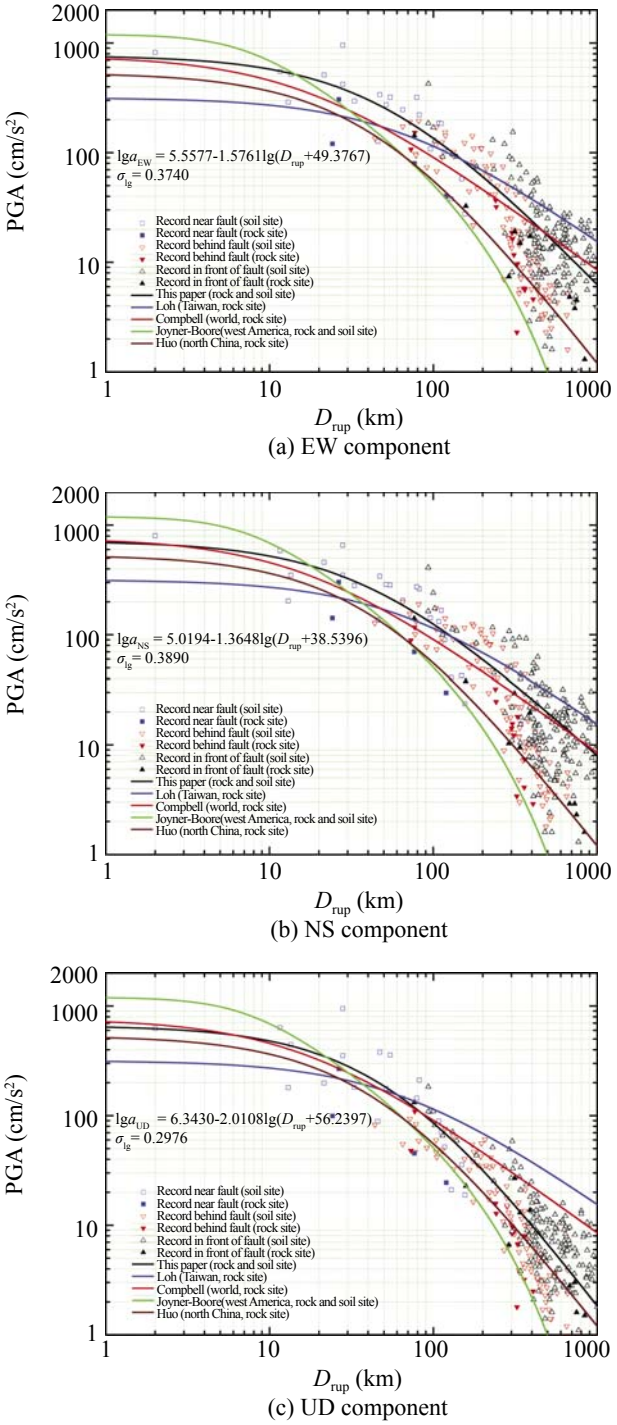

(a) EW component

(b) NS component

(c) UD component

Fig. 3 Attenuations of PGAs of different components

Since this earthquake had a mainly unilateral rupture, energy may have been focused in front of the fault, which generated a forward directivity effect and amplified the strong motion in front of the fault. The second reason is that stations located in the Weihe Basin were in front of the fault, which recorded much higher PGAs than those outside the basin due to a larger amplification of the soft soil in the basin.

For attenuations of the two horizontal components, it was found that as the fault distance became less than 20 km, Joyner-Boore's relationship was higher than observed in this event, and as the fault distance became greater than 150 km, Loh's relationship was higher than in this event. In other situations, attenuations from this event were higher than others. Note that since there were only a few stations located on rock sites, most of the records used to obtain the attenuations from this event were from soil sites. Joyner-Boore's relationship was obtained from rock and firm soil sites, where site conditions were very similar to this event. Compared to Joyner-Boore's relationship, the PGAs of this earthquake attenuated more slowly.

4 Hanging wall effect

According to source inversion and the field investigation, the Wenchuan earthquake was a dip-slip thrust faulting (Chen *et al.*, 2008; Wang *et al.*, 2008; Xu *et al.*, 2008). This type of earthquake, such as the 1994 Northridge and 1999 Chi-Chi earthquakes, always shows obvious hanging wall effects, which means that strong motions on the hanging wall were higher than on the foot wall. Therefore, it is important to study whether this large earthquake exhibited the hanging wall effect. According to the 4,150 data collected in the field investigation, an intensity isoseismal map of the Wenchuan earthquake was obtained (Yuan, 2008; see Fig. 2 in this reference). From the intensity isoseismal map, the intensity distribution showed no obvious hanging wall effect, and the earthquake damage was approximately symmetric around the fault surface rupture. The records from stations less than 100 km from the fault were used to determine whether the hanging wall effect occurred due to PGA, PGV and spectral accelerations in this earthquake.

If there were more available records and the stations were more uniformly distributed in the near-field region, more information on the characteristics of near fault strong motion would have been obtained. Unfortunately, from Fig. 2 and Table 1, it is seen that there were only 28 stations within 100 km from the fault, and the distribution of stations was not uniform. In particular, no station was located on the hanging wall less than 20 km from the fault, while in this region, strong motion on the hanging wall and foot wall would be very different according to studies from the Chi-Chi earthquake (Wang *et al.*, 2002). Therefore, only a preliminary study of the difference between strong motions on the hanging wall and foot wall more than 20 km from the fault can be made.

Figure 4 shows the attenuations of PGAs and PGVs in the near fault region. Note that in the area that was more than 20 km and less than 70 km from the fault, for both rock and soil sites, PGAs on the hanging wall were higher than on the foot wall at the same fault distance. This phenomenon was most prominent for the UD component. As the fault distance became greater than 70 km, the difference in the hanging wall and foot wall effect was not significant. The largest PGA of 957.4 cm/s^2 (the EW component of the Wolong station) was recorded on the hanging wall side. Therefore, it is suggested that in the Wenchuan earthquake, the hanging wall effect occurred with PGA.

For PGV between 20 km to 70 km from the fault, the values of parts of the records on the hanging wall were higher than on the foot wall at the same fault distance, whereas others were observed to be the reverse. The largest PGV (113 cm/s, fault normal component of Qingping station) was observed on the foot wall side. Therefore, the hanging wall effect may not have existed at PGV. Since the near fault region velocity time history always shows pulse type at components parallel and normal to the fault with higher PGV, the velocity time history of these two components were combined to obtain their PGV. Figure 5 shows the PGV of these two components with fault distance, where no hanging wall effect was observed.

The above results indicate that the hanging wall effect of this large earthquake may have been related to the frequency contents of strong motions, and only existed in some frequency bands. In order to further analyze these phenomena, the response spectra of periods 0.1 s, 0.5 s, 1.0 s, and 3.0 s of three components were compared, and the results are shown in Figs. 6–8. From these figures, it is seen that at period 0.1 s, the spectral accelerations on the hanging wall were higher than on the foot wall at the same fault distance, and at period 0.5 s, this phenomena also existed at most stations; however, as the periods increased to 1.0 s, this phenomena disappeared. At most stations at period 3.0 s, the spectral accelerations on the foot wall were higher than on the hanging wall. As the periods increased to more than 3.0 s, most spectral accelerations were less than 100 cm/s^2, which does not have much of an influence on structures; therefore, it is not discussed in this paper.

According to the above discussion, the hanging wall effect of this earthquake may have existed at periods of less than 0.5 s, and at high frequency. The intensity isoseismal map (Yuan, 2008) shows no obvious hanging wall effect, which may be related to the distribution of structural types with different natural periods near the fault. This phenomenon is different from the 1999 Chi-Chi earthquake, whose PGA, PGV and PGD on the hanging wall side were all much larger than on the foot wall side (Wang *et al.*, 2002), which means that the hanging wall effect existed in the long to short period range.

Table 1 Parameters of data from 28 near fault stations selected for this study

Station name	D_{rup} (km)	PGA (cm/s^2)			PGV (cm/s)					Spectral acceleration (cm/s^2)												Site condition	Hanging/ foot wall
										EW				NS				UD					
		EW	NS	UD	EW	NS	UD	FP	FN	0.1 s	0.5 s	1.0 s	3.0 s	0.1 s	0.5 s	1.0 s	3.0 s	0.1 s	0.5 s	1.0 s	3.0 s		
Wolong	28	957.4	655.8	948.1	51.5	38.8	20.4	60.9	31	1419.2	1513.8	349.7	51.0	1081.3	1009.3	257.1	39.1	2720.6	272.1	91.9	34.2	s	h
Lixiansb	82	221.3	261.7	211.1	9.1	7.2	9.6	7.5	9.5	745.15	140.2	31.4	24.5	1037.1	164.2	31.6	14.6	470.9	68.6	30.6	14.6	s	h
Lixianmk	54.5	321.5	283.9	357.8	19.5	15.7	12.9	19.2	19.4	681.42	641.9	185.6	36.2	685.4	554.8	104.8	21.15	1010.4	142.7	91.1	37.5	s	h
Lixiantp	47	339.6	342.1	379.6	17	12.6	13.1	16.9	13.8	1053.5	247.6	155.1	32.5	818.6	282.8	111.6	35.8	1619.7	171.0	93.0	26.9	s	h
Maoxiannx	28	421.1	349.4	352.5	27.3	23.2	19.3	23.8	25.8	844.49	980.9	250.6	62.4	1345.2	617.0	160.3	50.9	908.0	387.9	100.4	43.0	s	h
Maoxiandx	65	246.6	206.5	143.9	17	31.8	11.1	26.2	23	331.2	719.5	388.5	20.9	280.2	595.9	955.9	30.8	248.7	333.7	93.3	23.1	s	h
Pingwumz	51.5	273.8	287.4	177.4	10.7	19.1	11.4	13.1	19.6	790.39	166.4	46.4	35.2	515.2	537.0	129.3	34.4	383.4	77.03	68.5	27.8	s	h
Jiuzaigy	100	169.7	241.4	109.3	10	8.3	8	9.9	11.3	633.09	241.2	51.3	15.3	603.6	167.9	45.3	15.3	329.8	103.2	24.9	12.0	s	h
Wudu	93	185	163.9	108.7	16.5	12.1	10.5	17	15.2	360.05	457.8	346.1	27.1	360.6	207.1	200.1	18.2	394.9	154.5	71.7	15.1	s	h
Maoxiandb	26.5	306.5	302.1	266.6	22.6	19.2	12.9	22.6	21	784.79	862.7	177.1	34.2	873.2	317.3	139.2	66.8	697.9	191.6	104.7	37.1	r	h
Wenxian	76.5	142.6	141.1	131.9	11.1	9.3	10.2	10.6	11	213.75	72.0	81.9	32.4	269.5	59.1	88.2	20.8	217.4	93.7	67.0	23.4	r	h
Pixianzxs	24.2	120.6	142.3	99.2	19.2	18.7	17.6	16.8	21.6	135.93	212.4	198.8	64.6	153.4	435.8	216.5	64.3	170.9	161.2	160.8	62.2	r	f
Chengduzh	76.5	79.8	69.7	45.3	16.3	10	10.9	11.2	17.6	139.48	125.7	103.4	39.4	182.8	87.6	91.16	33.3	84.1	64.8	52.2	53.0	r	f
Xinjinlh	73	107.6	89.1	48	16.3	10.4	9	12.2	13	205.89	149.4	123.7	53.4	265.9	105.8	64.4	24.4	76.0	68.4	57.6	40.4	r	f
Qingping	2	824.3	802.5	622.9	103.1	58	39.7	113	37.8	2312.8	1008.7	538.8	266.9	1633.3	812.1	398.6	191.4	1404.3	526.7	240.3	105.4	s	f
Bajiao	11.6	548.9	585.7	632.9	62.4	69.7	43.9	59.3	57.1	703.39	1324.8	538.7	79.4	1062.9	1123.6	730.4	109.0	2182.7	390.4	375.4	90.3	s	f
Anxiants	13	289.3	203.4	179.9	26.4	31.2	26.7	26.6	31.2	480.83	605.9	238.1	119.8	495.6	389.2	290.4	159.8	177.5	256.2	227.0	114.0	s	f
Deyangbm	45.8	126.5	136.3	88.9	23.4	36.1	31.4	22.1	30.7	281.43	245.6	262.6	69.4	246.5	239.9	156.0	90.8	123.1	132.5	154.6	71.2	s	f
Jiangyouhz	13.5	519.3	350.1	444.3	20.1	31	22.8	27	20.7	1307.1	415.9	163.2	48.4	1553	319.6	181.8	96.1	844.8	181.3	104.8	54.07	s	f
Jiangyoudzt	21.5	511.8	458.8	198.2	26.2	36.7	33.7	33.5	29.8	787.91	528.4	293.9	88.3	861.9	333.0	314.6	98.5	547.1	284.5	218.2	70.2	s	f
Jiangyouch	33	296.8	281.4	180.5	22.3	36.8	22.4	30.7	24.8	470.25	856.4	273.8	78.3	497.8	565.7	447.2	93.1	373.9	317.1	239.0	61.1	s	f
Guangyuanzj	93	424.4	410.6	183.3	23.5	43.2	23.4	34.8	37.1	577.56	853.3	288.2	54.0	627.2	957.2	237.7	55.2	316.8	306.2	85.8	36.4	s	f
Guanyuansj	79	320.7	273.9	143.7	20.5	22.7	18.1	25.8	16.9	636.35	324.3	165.0	37.8	575.1	286.3	160.0	51.4	348.9	151.1	112.3	40.0	s	f
Cangxiqxj	112	184.8	166.9	69.9	25.1	12.9	8.2	20	15.8	431.92	245.8	189.4	60.9	343.0	243.1	160.6	34.9	162.0	101.9	106.0	26.2	s	f
Dayiyp	44	135.1	127.6	82.7	28.4	17.2	13.9	23.9	19.9	256.28	286.5	182.7	62.1	245.5	281.5	164.6	46.9	136.4	132.3	129.8	44.3	s	f
Pujiangwx	77.5	97.7	101.2	46.9	19.4	9.9	13.5	14.2	14.3	194.5	217.3	138.0	37.3	190.0	146.2	122.2	37.2	80.8	62.2	79.6	42.3	s	f
Pujiangdx	81.5	195.8	190.3	59	16.3	14.8	10.3	16.7	13.3	241.82	353.2	118.6	34.5	260.2	464.4	82.3	28.1	103.0	67.0	56.1	23.7	s	f
Qiaolaiyz	65	173.8	199.8	55.1	14.4	8.4	10	12.3	10.4	639.39	217.7	96.6	24.6	555.4	158.1	114.8	20.1	119.7	111.6	97.2	22.5	s	f

Notes: In the table symbols D_{rup} denotes the rupture distance; s and r represents soil and rock sites, respectively.

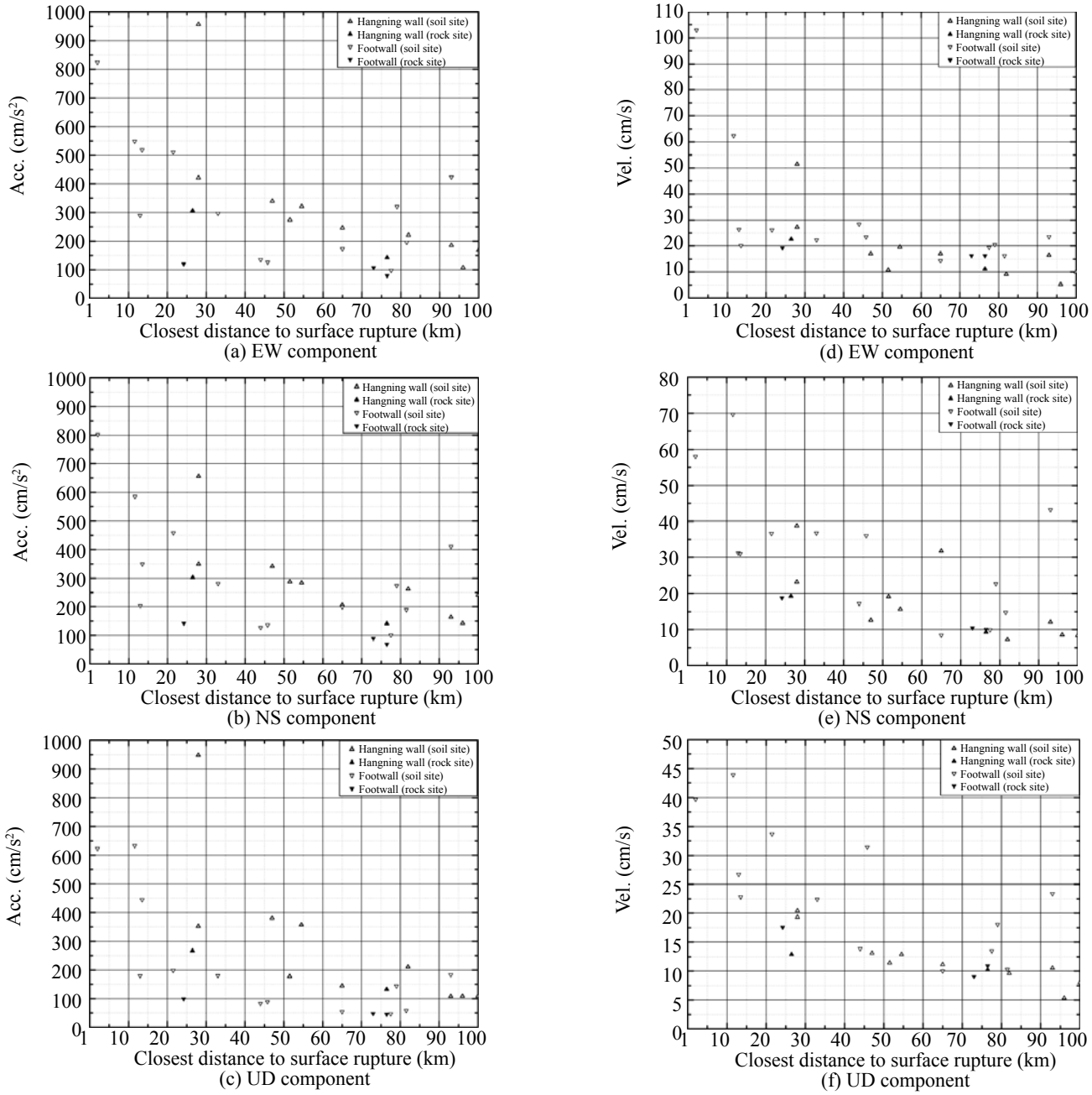

Fig. 4 Comparison of the PGA (left) and PGV (right) on the hanging and the foot wall

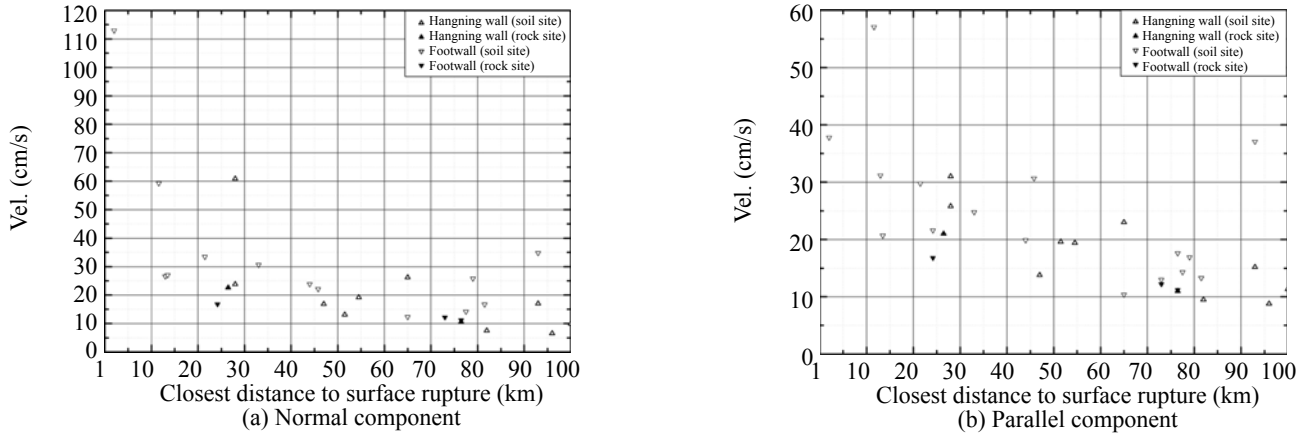

Fig. 5 Comparison of the PGV on the hanging and the foot walls at fault parallel (right) and normal (left) components

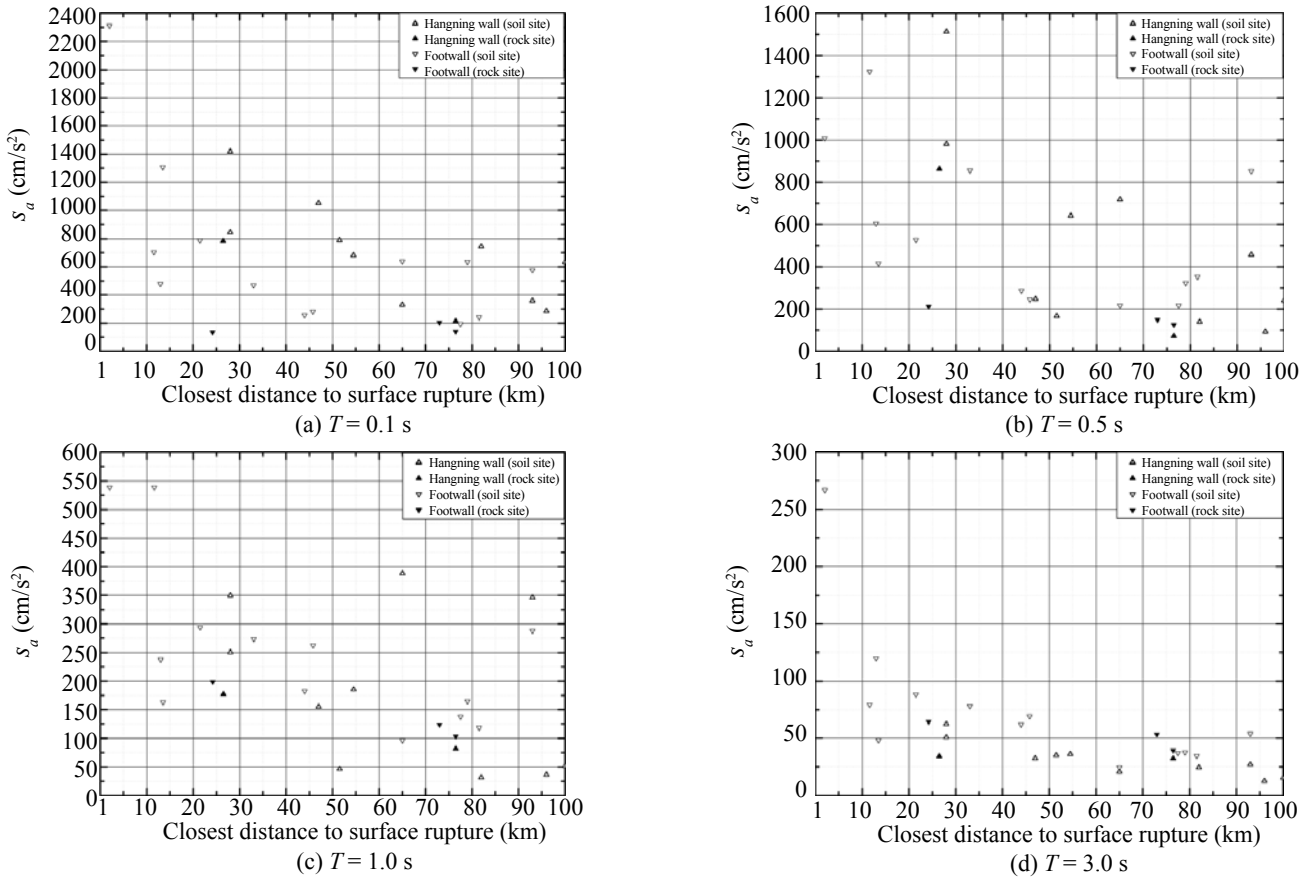

Fig. 6 Comparison of the spectral acceleration on the hanging and foot walls at periods 0.1 s, 0.5 s, 1.0 s and 3.0 s of EW component

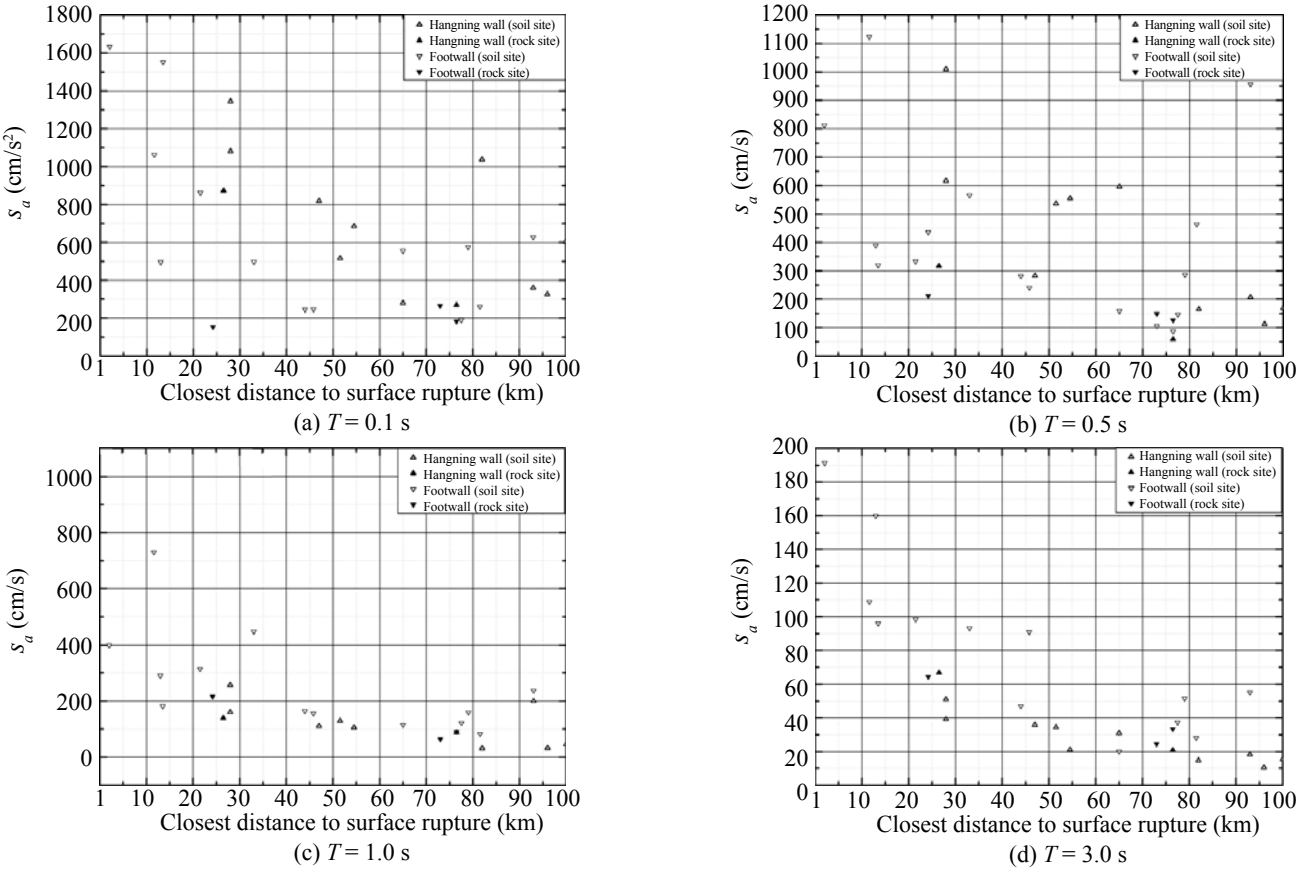

Fig. 7 Comparison of the spectral acceleration on the hanging and foot walls at periods 0.1 s, 0.5 s, 1.0 s and 3.0 s of NS component

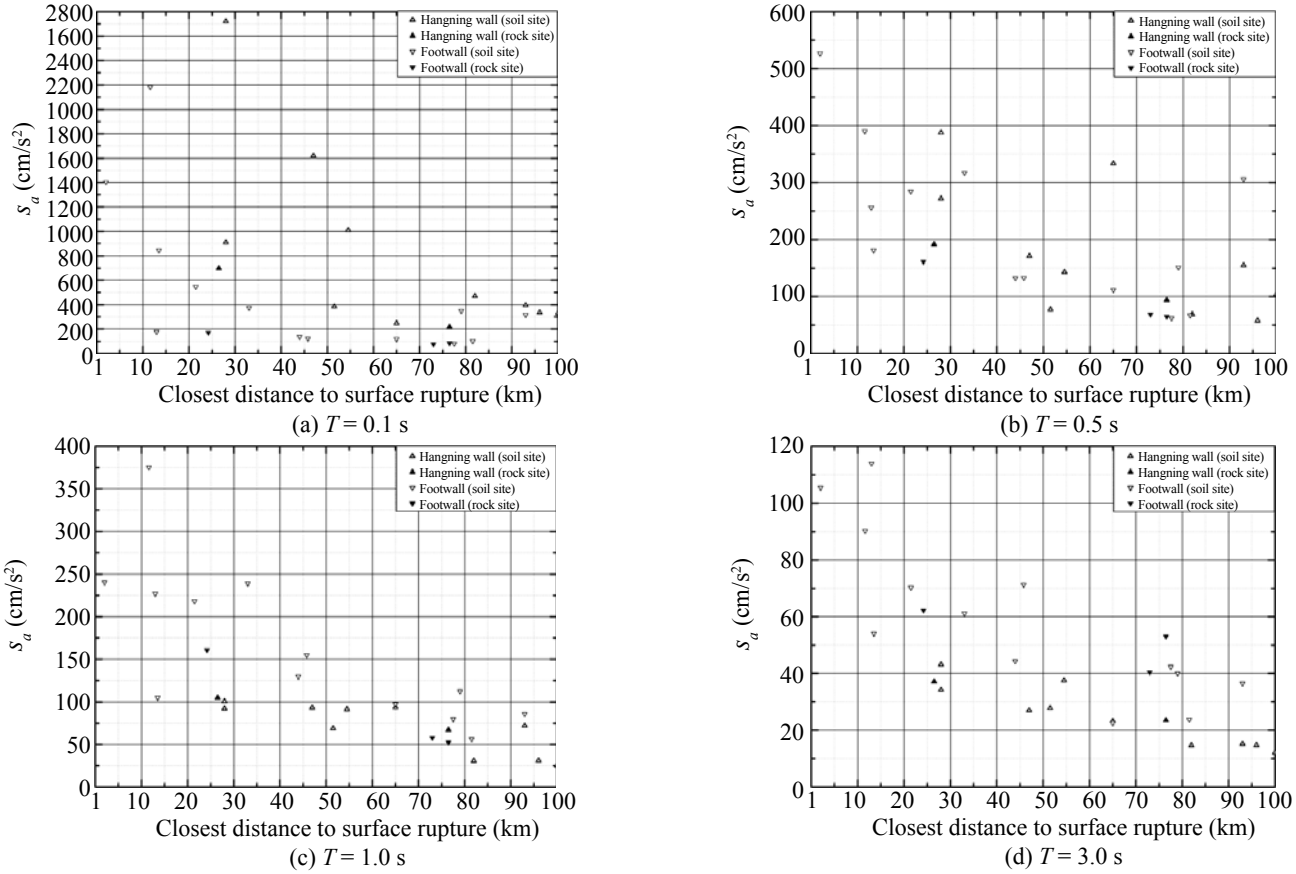

Fig. 8 Comparison of the spectral acceleration on the hanging and foot walls at periods 0.1 s, 0.5 s, 1.0 s and 3.0 s of UD component

Note that the difference in ground motions between the hanging wall and foot wall depends not only on the fault type, but also on local site conditions. Only preliminary conclusions are obtained in this study from relatively few records and without considering local site conditions; therefore, further research should be conducted to obtain more detailed results.

5 Characteristics of velocity pulses

Near fault strong motion always contains distinct pulses in velocity time histories, especially for components normal and parallel to a fault in regions very near to the fault.

First, records from the Qingping station are discussed. These were only about 2 km from the fault, the closest stations to the surface rupture. Figure 9 shows the velocity time histories of EW, NS, FN (fault normal), FP (fault parallel) and UD components, where the time histories of all five components showed an obvious velocity pulse. The largest pulse peak was 113 cm/s, which was on the fault normal component, while the smallest one was 40 cm/s, which was on the UD component. From the velocity Fourier amplitude spectra, the prominent velocity periods were in the range of 5.0 s–10.0 s.

Next, the records from Wolong station were investigated. The PGA of the EW component was 957.4 cm/s^2, the largest PGA observed in the records from this earthquake. The fault distance of this station was 28 km, relatively far from the surface rupture. Figure 10 shows the velocity time histories of records from the Wolong station, where it was seen that the time histories were generated by at least two events. From the EW, NS and FN components, no obvious velocity pulse was observed; but from FP and UD components, there was obviously a velocity pulse at both events, and the velocity peaks were 30 cm/s and 20.4 cm/s for these two components. From the velocity Fourier amplitude spectra, prominent velocity periods were found to be in the range of 5.0 –10.0 s.

The closest 10 stations to the surface rupture were selected to further study the velocity pulse. Figure 11 shows the velocity time histories of the FN, FP and UD components, where the PGV and fault distance are also shown. From these figures, most time histories were found to have a velocity pulse. The peaks of the velocity pulses in most stations were less than 50 cm/s, except for the Qingping, Bajiao, and Wolong stations. Compared with the 1999 Chi-Chi earthquake, the peaks of the velocity pulses were relatively smaller. Therefore, it is important to study why this large earthquake generated small velocity pulses.

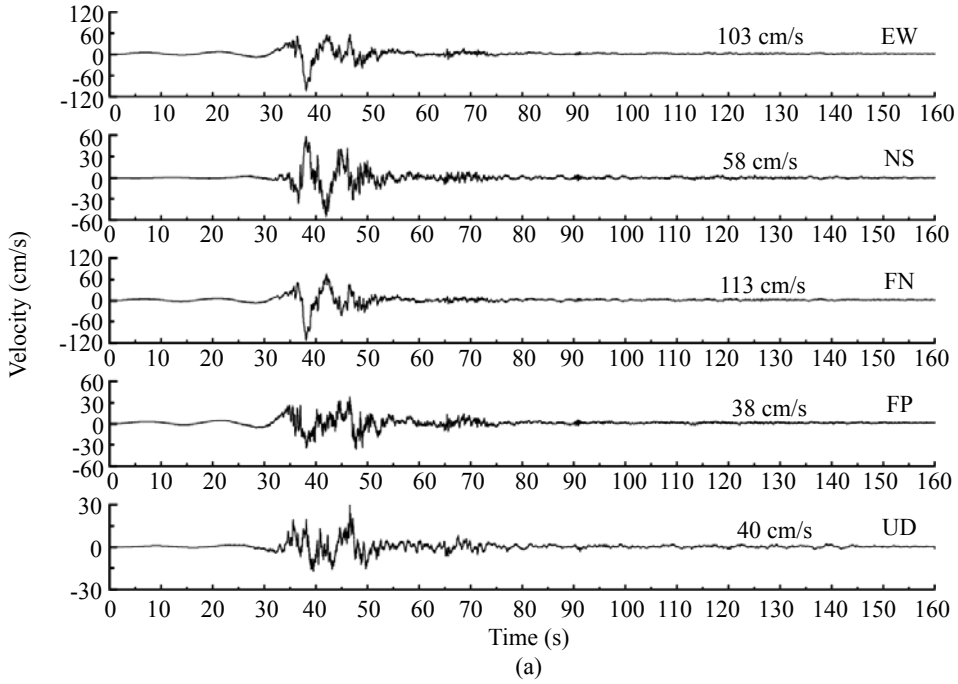

(a)

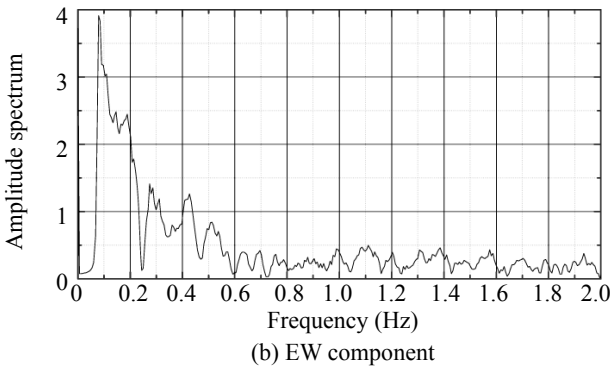

(b) EW component

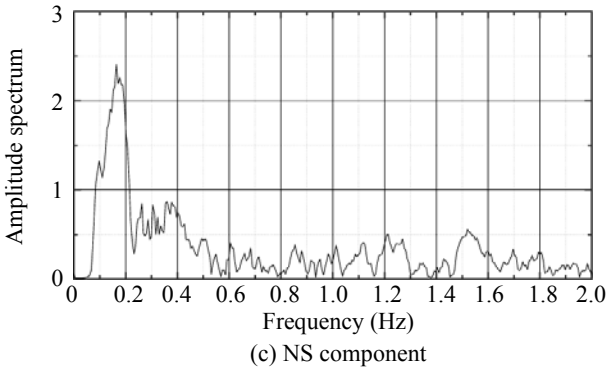

(c) NS component

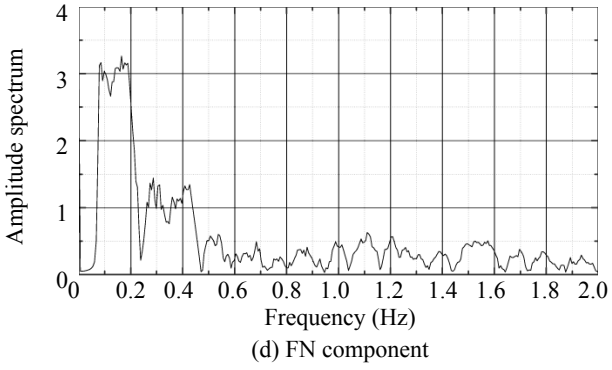

(d) FN component

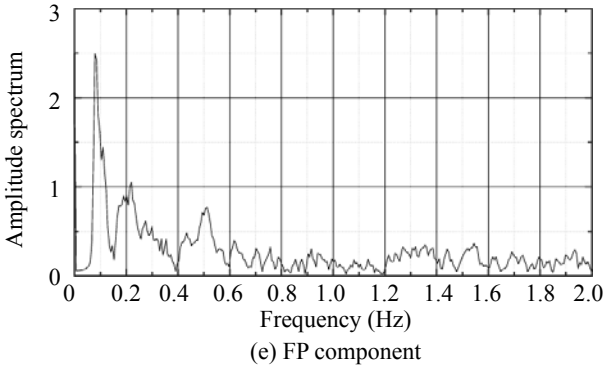

(e) FP component

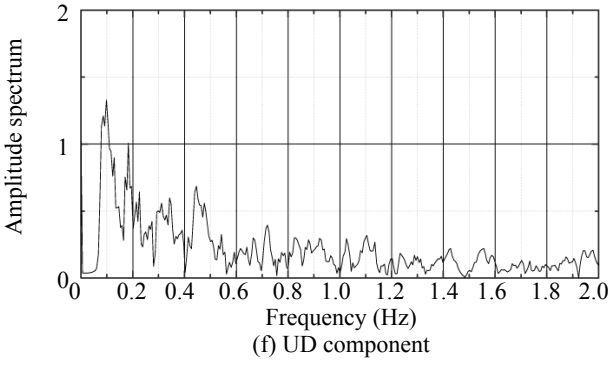

(f) UD component

Fig. 9 Velocity time histories (a) and their Fourier amplitude spectra (b)–(f) at Qingping station

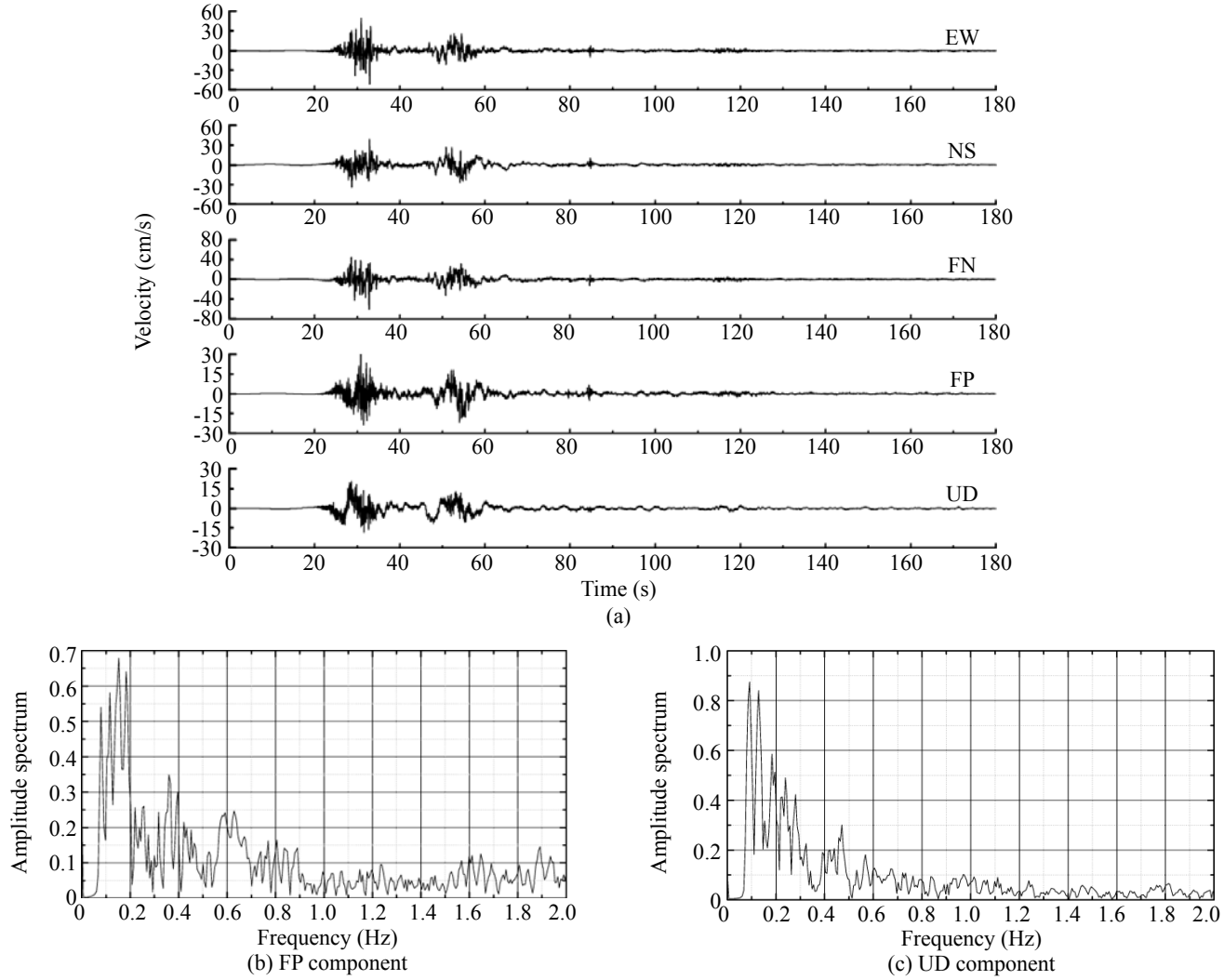

Fig. 10 Velocity time histories (a) and their Fourier amplitude spectrum (b)–(c) at Wolong station

Although many pulse peaks were smaller than in the Chi-Chi earthquake, at stations very near the fault such as the Qingping station, the peak of velocity pulse was still over 100 cm/s. The velocity pulses may cause major damage to long period structures, so it is still important to study the velocity pulses of this earthquake. Only a simple analysis is provided in this paper; the relationship of the pulse to the fault rupture process and site conditions should be studied further.

6 High UD component and its relationship to the hanging/foot wall

This earthquake also shows larger PGA of the UD component. For example, the PGA of the UD component was 948.1 cm/s^2 at Wolong station, a little smaller than the EW component (957.4 cm/s^2), but larger than the NS component (655.8 cm/s^2). The records from 28 near fault stations and the ratio of vertical component to horizontal component a_V/a_H were used in the analysis, where a_V is the PGA of the vertical component, and a_H is of the PGA of the two horizontal components. Figure 12 shows the PGA ratio of the UD component to the two horizontal components, where the left figure is the hanging wall and the one on the right corresponds to the foot wall.

An important phenomenon was observed; that is, the ratio of the hanging and foot wall were very different. On the hanging wall, less than 100 km from the fault, the ratios from most stations were larger than 2/3 (Fig. 12, left), which means that this earthquake generated larger PGA of UD across relatively broad regions. However, on the foot wall, as the fault distance became more than 25 km, the ratios of most stations were smaller than 2/3, which means that the larger PGA of the UD component only existed in a very narrow region. This phenomenon indicates that during the earthquake, the hanging wall may move more strongly than the foot wall at the UD component. Note that this conclusion was made without considering the local site conditions. Therefore, further research should be conducted to determine whether the characteristics of the strong motions mentioned above are related to local site conditions.

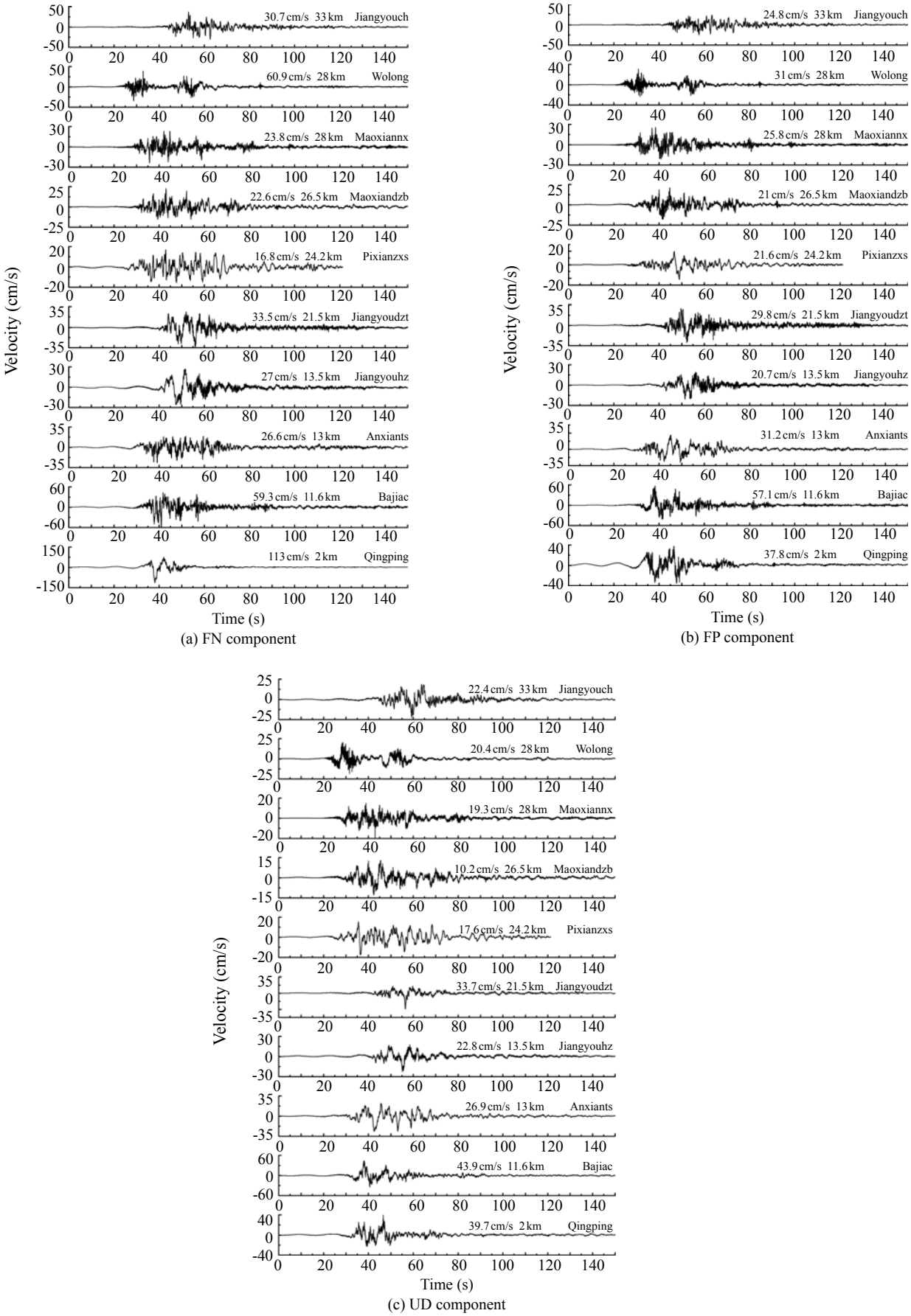

Fig. 11 Velocity time histories of FN, FP and UD components at the 10 stations closest to the surface rupture

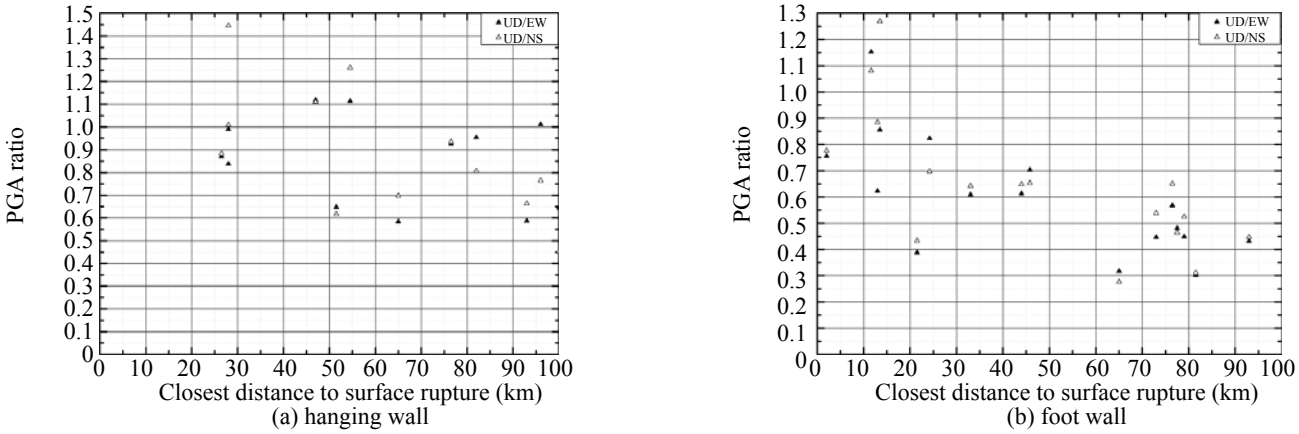

Fig. 12 PGA ratio of UD component to the EW and NS components on the hanging and foot wall

7 Conclusion

Using the strong motion data from 5.12 Wenchuan earthquake, the attenuations, hanging wall effect and velocity pulse of the earthquake are studied in this paper. Some preliminary results were obtained as follows:

(1) Compared to Joyner-Boore's relationship, where site conditions were closer to recording stations, the PGA of this earthquake attenuated more slowly. The EW component attenuated a little more rapidly than the NS component.

(2) The hanging wall effect of this earthquake was obvious on PGA but disappeared at PGV, and it may have existed at periods less than 0.5 s. It was different from the 1999 Chi-Chi earthquake, whose PGA, PGV and PGD on the hanging wall side were all much larger than on the foot wall side.

(3) Most records at stations less than 30 km from the fault showed velocity pulses, especially in the very near fault region. The peaks of the velocity pulses at most stations were less than 50 cm/s, smaller than in the 1999 Chi-Chi earthquake. At stations very near the fault, the peaks of the velocity pulses were still over 100 cm/s, which may cause major damage to long period structures.

(4) This earthquake also showed larger PGA on the UD component, and it behaved very different on the hanging wall and the foot wall. On the hanging wall less than 100 km from the fault, the ratios at most stations were bigger than 2/3, whereas on the foot wall, the ratios at most stations were smaller than 2/3 as the fault distance became more than 25 km.

Note that this preliminary study, especially regarding the near-fault strong motion characteristics, was based on limited records from an extremely non-uniform distribution of stations, and the impact of local site conditions was ignored. All these factors may significantly influence the conclusions. Therefore, an extensive study should be conducted that uses more available data.

Acknowledgement

The authors are grateful to the National Strong Motion Networks and all the managers and experts who provided the records used in this study. The research work was also supported by the National Natural Science Foundation of China (90715038), the National Basic Research Program of China (2007CB71420) and Basic Science & Research Foundation of Institute of Engineering Mechanics, CEA (2006A02). This support is gratefully acknowledged.

Reference

Campbell KW (1981), "Near-source Attenuation of Peak Horizontal Acceleration," *Bull. Seis. Soc. Am.*, **71**(6): 2039–2070.

Chen YT, Xu LS, Zhang Y, Du HL, Feng WP, Liu C and Li CL (2008), "Analysis of the Source Characteristics of the Wenchuan Earthquake of May 12, 2008," *Report by the Institute of Geophysics* (http://www.cea-igp.ac.cn), China Earthquake Administration, on the Wenchuan Earthquake. (in Chinese)

Hu YX (1999), *The Technique of the Evaluation of Seismic Safety*, Beijing: Seismological Press.

Huo JR (1989), "Study on the Attenuation Laws of Strong Earthquake Ground Motion Near the Source," *Ph.D Thesis*, Institute of Engineering Mechanics, China Earthquake Administration. (in Chinese)

Joyner W and Boore D (1981), "Peak Horizontal Acceleration and Velocity from Strong-motion Records Including Records from the 1979 Imperial Valley, California, Earthquake," *Bull. Seism. Soc. Am.*, **71**(3): 2011–2038.

Li XJ, Zhou ZH *et al*. (2008a), "Preliminary Analysis of Strong Motion Recordings from the Magnitude 8.0 Wenchuan, China Earthquake of May 12, 2008," *Seismological Research Letters*, **79**(6): 844–854.

Li XJ, Zhou ZH *et al*. (2008b), "Strong Motion Observations and Recordings from the Great Wenchuan Earthquake," *Earthquake Engineering and Engineering Vibration*, **7**(3): 235–246

Wang WM, Zhao LF, Li J *et al.* (2008), "Rupture Process of the M_s 8.0 Wenchuan Earthquake of Sichuan, China," *Chinese J. Geophysics*, **51**(5): 1403–1410. (in Chinese)

Wang QQ, Zhou XX, Zhang PZ *et al*. (2002), "Characteristic of Amplitude and Duration for Near Fault Strong Ground Motion from the 1999 Chi-Chi, Taiwan Earthquake," *Soil Dynamic and Earthquake Engineering*, **22**(1): 73–96.

Xu XW, Wen XZ, Yu Shen'e *et al*. (2008), "Discovery of the Wenchuan *M*8.0 Earthquake Surface Ruptures and Discussion for Its Seismogenic Structure," Seismology and Geology, **30**(3): 894–926. (in Chinese)

Yuan YF (2008), "Loss assessment of Wenchuan," *Earthquake Engineering and Engineering Vibration*, **28**(5): 10–19. (in Chinese)